Published in final edited form as:
Toxicol Appl Pharmacol. 2012 July 15; 262(2): 156–166. doi:10.1016/j.taap.2012.04.030.

Rapid generation of mitochondrial superoxide induces mitochondrion-dependent but caspase-independent cell death in hippocampal neuronal cells that morphologically resembles necroptosis☆

Masayuki Fukui, **Hye Joung Choi**, and **Bao Ting Zhu***
Department of Pharmacology, Toxicology and Therapeutics, School of Medicine, University of Kansas Medical Center, Kansas City, KS 66160, USA

Abstract

Studies in recent years have revealed that excess mitochondrial superoxide production is an important etiological factor in neurodegenerative diseases, resulting from oxidative modifications of cellular lipids, proteins, and nucleic acids. Hence, it is important to understand the mechanism by which mitochondrial oxidative stress causes neuronal death. In this study, the immortalized mouse hippocampal neuronal cells (HT22) in culture were used as a model and they were exposed to menadione (also known as vitamin K_3) to increase intracellular superoxide production. We found that menadione causes preferential accumulation of superoxide in the mitochondria of these cells, along with the rapid development of mitochondrial dysfunction and cellular ATP depletion. Neuronal death induced by menadione is independent of the activation of the MAPK signaling pathways and caspases. The lack of caspase activation is due to the rapid depletion of cellular ATP. It was observed that two ATP-independent mitochondrial nucleases, namely, AIF and Endo G, are released following menadione exposure. Silencing of their expression using specific siRNAs results in transient suppression (for ~12 h) of mitochondrial superoxide-induced neuronal death. While suppression of the mitochondrial superoxide dismutase expression markedly sensitizes neuronal cells to mitochondrial superoxide-induced cytotoxicity, its over-expression confers strong protection. Collectively, these findings showed that many of the observed features associated with mitochondrial superoxide-induced cell death, including caspase independency, rapid depletion of ATP level, mitochondrial release of AIF and Endo G, and mitochondrial swelling, are distinctly different from those of apoptosis; instead they resemble some of the known features of necroptosis.

Keywords

ATP-independent neuronal death; Caspase-independent neuronal death; Necrosis; Mitochondrial damage-induced cell death; Superoxide dismutase; Reactive oxygen species; Apoptosis-inducing factor; Endonuclease G

☆This study was supported by funds from the University of Kansas Endowment and from the NIH (grant number ES015242).

*Corresponding author at: Department of Pharmacology, Toxicology and Therapeutics, School of Medicine, University of Kansas Medical Center, Room 4061 of HLSIC Building, 2146 W. 39th Street, Kansas City, KS 66160, USA. Fax: +1 913 588 8356. BTZhu@kumc.edu. .

Conflict of interest statement The authors have no conflict of interests to declare. The sponsors had no involvement in the study design; collection, analysis and interpretation of data; writing of the manuscript; and decision to submit the manuscript for publication.

Introduction

Although the brain only accounts for roughly 2% of the total body weight, it utilizes approximately 20% of total body oxygen intake (Clark et al., 1999). It is estimated that 1–3% of mitochondrial oxygen consumed during the process of oxidative phosphorylation is incompletely reduced, which results in the formation of superoxide anion, a predominant form of reactive oxygen species (ROS) produced in mitochondria (Chance et al., 1979; Kudin et al., 2004). In recent years, there is emerging evidence suggesting that elevated mitochondrial superoxide production is a contributing factor in the etiology of neurodegenerative diseases, including Parkinson's disease, Alzheimer's disease (AD), and amyotrophic lateral sclerosis (Coyle and Puttfarcken, 1993; Halliwell, 1992; Lin and Beal, 2006; Maier and Chan, 2002; Sompol et al., 2008). ROS causes neuronal damage through oxidative modifications of cellular lipids, proteins, and nucleic acids (Trushina and McMurray, 2007). Recent studies indicate that oxidative damage is a common early event in the brains of AD patients, occurring well before the onset of significant pathology and clinical symptoms (Nunomura et al., 2001; Smith et al., 1996).

A number of earlier studies have suggested that menadione (2-methyl-1,4-naphthoquinone; vitamin K_3) is a superoxide generator, which induces the production of superoxide inside the cells *via* one-electron transfer reactions (Iyanagi and Yamazaki, 1970; Thor et al., 1982; White and Clark, 1988). In addition, metabolism of menadione by the one-electron reducing enzymes, such as microsomal NADPH-dependent cytochrome P450 reductase and mitochondrial NADH-dependent ubiquinone oxidoreductase, generates an unstable semi-quinone radical (Criddle et al., 2006; Iyanagi and Yamazaki, 1970), and its reverse oxidation generates superoxide when molecular oxygen is present. Superoxide formation and accumulation induced by menadione reduce the cellular antioxidant capacity and subsequently induce cell death. Partly because of menadione's ability to induce superoxide formation and oxidative stress, a number of studies in recent years have also explored its potential anticancer effects (Lamson and Plaza, 2003).

Since superoxide accumulation and oxidative stress play an important role in the initiation and progression of neurodegenerative diseases, it is important to better understand the mechanism underlying oxidative stress-induced neuronal cell death. In many *in vitro* mechanistic studies, the exogenous free radical-generating systems, *e.g.*, through the addition of hypoxanthine/xanthine oxidase or hydrogen peroxide to the cell culture medium, are often used as models of oxidative stress. However, the cellular effects of ROS generated outside a cell may differ considerably from the ROS generated inside a cell. Partly because of this consideration, the present study chose to employ an *in vitro* oxidative stress model by exposing cultured HT22 neuronal cells to menadione to increase superoxide formation inside the cells. HT22 cells are immortalized mouse hippocampal neuronal cells that have become a commonly-used *in vitro* experimental model for studying oxidative stress-induced neuronal death in recent years (Behl et al., 1997; Maher and Davis, 1996; Xu et al., 2007). By using this model, we found that exposure of neuronal cells to menadione causes selective accumulation of superoxide in the mitochondria, along with rapid development of mitochondrial dysfunction and cellular ATP depletion. We also demonstrated that many of the observed features associated with mitochondrial superoxide-induced cell death, including caspase independency, rapid depletion of cellular ATP level, mitochondrial release of AIF and Endo G, and mitochondrial swelling, are distinctly different from those of apoptosis; instead they resemble the features of necroptosis.

Materials and methods

Chemicals and reagents

Dulbecco's modified Eagle's medium (DMEM), fetal bovine serum (FBS), trypsin-EDTA solution (containing 0.5 g/L trypsin and 0.2 g/L EDTA), and menadione were purchased from Sigma-Aldrich (St. Louis, MO). The antibiotic solution (containing 10,000 U/mL penicillin and 10 mg/mL streptomycin) was obtained from Gibco (Invitrogen, Grand Island, NY). All antibodies were purchased from Cell Signaling Technology (Beverly, MA). All inhibitors were purchased from Calbiochem (La Jolla, CA).

Cell culture and treatment

HT22 murine hippocampal neuronal cells were a gift from Dr. David Schubert (Salk Institute, La Jolla, CA), maintained in DMEM supplemented with 10% (*v/v*) fetal bovine serum (FBS) and antibiotics (penicillin–streptomycin), and incubated at 37 °C under 5% CO_2. Cells were sub-cultured once every 2 days. Cells were seeded in 96-well plates at a density of 5000 cells per well. The stock solution of menadione (40 mM in DMSO; dimethyl sulfoxide) or etoposide (50 mM in DMSO) was diluted in the culture medium immediately before addition to each well at the desired final concentrations, and the treatment usually lasted for 24 h.

MTT assay

As an initial assessment of cell viability, the MTT assay was used. After the cultured neuronal cells were incubated in 96-well plates with menadione or other toxicants for desired lengths of time, 10 μL MTT (at 5 mg/mL) was added to each well at a final concentration of 0.5 mg/mL, and the mixture was further incubated for 1 h, and the liquid in the wells was removed thereafter. DMSO (100 μL) was then added to each well, and the absorbance was read with a UV max microplate reader (Molecular Device, Palo Alto, CA) at 560 nm. The relative cell viability was expressed as the percentage of the control that was treated with vehicle only.

Western blotting

For Western blotting, cells were washed first with PBS, and then suspended in 100 μL lysis buffer (containing 20 mM Tris–HCl, 150 mM NaCl, 1 mM EDTA, 1% Triton X-100, the protease inhibitor cocktail, 2 mM Na_3VO_4, and 10 mM NaF, pH 7.5). The amount of proteins was determined using the Bio-Rad protein assay (Bio-Rad, Hercules, CA). An equal amount of proteins was loaded in each lane. The proteins were separated by 10% SDS-polyacrylamide gel electrophoresis (SDS-PAGE) and then electrically transferred to the polyvinylidene difluoride membrane (Bio-Rad). After blocking the membrane using 5% skim milk, caspase-3, PARP, AIF, cytochrome *c*, and MAPKs were immuno-detected individually using specific primary antibodies obtained from Cell Signaling Technology (Beverly, MA). Thereafter, the horseradish peroxidase (HRP)-conjugated anti-rabbit IgG was applied as the secondary antibody, and the positive bands were detected using Amersham ECL plus Western blotting detection reagents (GE Healthcare, Piscataway, NJ).

Flow cytometric analysis

After treatment with menadione, cells were harvested by trypsinization and washed once with phosphate-buffered saline (PBS), pH 7.4. After centrifugation, cells were stained with propidium iodide (PI) for analysis of cell cycles, or double-stained with annexin V and PI using the annexin V-FITC apoptosis detection kit (BD Biosciences, San Jose, CA) for analysis of the translocation of phosphatidylserine (PS) from the inner leaflets to the outer leaflets of the plasma membrane, or stained with 3,3′-dihexyloxacarbocyanine iodide

[$DiOC_6(3)$; Molecular Probes, Eugene, OR] for analysis of the mitochondrial membrane potential (MMP). For cell cycle analysis, cells were resuspended in 1 mL of 0.9% NaCl, and fixed with 2.5 mL of ice-cold 90% ethanol. After incubation at room temperature for 30 min, cells were centrifuged and the supernatant was removed. Cells were resuspended in 1 mL of PBS containing 50 μg/mL PI and 100 μg/mL ribonuclease A and incubated at 37 °C for 30 min. For annexin V-PI staining, the procedure was carried out according to the protocols of the manufacturer. For MMP analysis, cells were resuspended in 1 mL of culture medium containing 25 nM of $DiOC_6(3)$ and incubated at 37 °C for 15 min. After centrifugation, cells were resuspended in PBS. All flow cytometric analyses were performed on the BD LSR II (BD Bioscience, San Jose, CA).

Measurement of mitochondrial superoxide formation

For mitochondrial superoxide detection, cells were stained with MitoSOX Red (Molecular Probes) according to the protocols provided by the manufacturer. Accumulation of the mitochondrial superoxide was observed and photographed under a fluorescence microscope (AXIO, Carl Zeiss Corporation, Germany). To quantify the amount of mitochondrial superoxide, flow cytometric analysis was performed. MitoSOX Red was excited by laser at 488 nm and data were collected at 585/42 nm (FL2) as described earlier (Fukui and Zhu, 2010).

Analysis of subcellular morphology by transmission electron microscopy (TEM)

Cells were harvested using trypsin-EDTA and fixed in 2% glutaral-dehyde for 4 h, and centrifuged to form pellets. Sample preparation was carried out according to a previously-described method (Hanaichi et al., 1986). Briefly, the pellets were rinsed in 0.1 M cacodylate buffer (purchased from Electron Microscopy Sciences [EMS], Hatfield, PA) and post-fixed in 1% osmium tetroxide (EMS). Cell pellets were dehydrated through a graded series of ethanol and then passed through a propylene oxide twice and lastly placed in propylene oxide/Embed 812 resin (EMS) overnight for infiltration, and then polymerized in a 60 °C oven overnight. Sections were cut on a Leica UCT ultra microtome at 80 nm using a Diatome diamond knife. Sections were contrasted with uranyl acetate and Sato's lead citrate (EMS), and viewed and photographed on a JEOL 100CXII TEM at 60 kV (J.E.O.L. Ltd., Tokyo, Japan).

Nuclear staining

Nuclear morphology of HT22 cells was visualized using a fluorescence microscope after the cells were stained with 2 μM Hoechst-33342 and 10 μg/mL PI in DMEM (without FBS) at 37 °C for 10 min. Morphological changes were photographed with a built-in camera.

Construction of SOD1 or SOD2 stable knockdown in HT22 cells

The control shRNA plasmid (sc-108060), SOD1 shRNA plasmid (sc-36522-SH), and SOD2 shRNA plasmid (sc-41656-SH) were purchased from Santa Cruz Biotechnology. The control shRNA plasmid encodes a scrambled shRNA sequence that would not lead to specific degradation of any known cellular mRNAs. The SOD1 shRNA plasmid and SOD2 shRNA plasmid carry the puromycin resistance gene for the ease of isolating shRNA plasmid DNA-transfected cells. Transfection of shRNA plasmids was carried out using Lipofectamine-2000 (Invitrogen) according to the protocols of the manufacturer.

Construction of the SOD2 stable over-expression in HT22 cells

The pEGFP-N1/SOD2 plasmid was a generous gift provided by Dr. Sonia Flores, at the Division of Pulmonary Sciences and Critical Care Medicine, University of Colorado (Denver, CO, USA). HT22 cells were transfected with the pEGFP-N1/SOD2 plasmid as

described by Connor et al. (2005) using Lipofectamine-2000. Although the pEGFP-N1/SOD2 plasmid had a neomycin-resistant gene, we found that HT22 cells were also strongly resistant to neomycin. Therefore, we could not use neomycin for selection of transfected cells. To establish the stably-transfected cells, we collected the GFP-positive cells using FACS Aria II (BD Bioscience). After three times of cell sorting, the population of GFP-positive cells was increased to approximately 77%. Then, the transfected cells were seeded in 96-well culture plate at 1 cell per well. After 2 weeks of culture, single colony was harvested for determination of the SOD2-GFP fusion protein level by Western blotting. Mitochondria and cytosol were fractionated using the Mitochondria/Cytosol Fractionation Kit (Bio Vision, Mountain View, CA, USA), and the SOD activity was then determined using the Superoxide Dismutase Activity Assay Kit (Bio Vision). In the SOD2 over-expressed cells, the cytosolic SOD activity was 116.8±5.5% and the mitochondrial SOD activity was 201.4±12.2% compared to the corresponding SOD activity present in the mock plasmid-transfected control cells.

Analysis of cellular ATP levels

The cellular ATP levels were determined using the ApoSENSOR™ cell viability assay kit (Bio Vision). The cellular ATP levels were normalized by cellular protein and shown as a ratio to the corresponding levels in control cells (set at 100%).

Data analysis

Wherever possible, data were expressed as mean±S.D. (standard deviation). Statistical significance was determined using the analysis of variance (*ANOVA*) followed by a multiple comparison test with a Dunnett's test (SPSS software). *P* value of less than 0.05 was considered statistically significant.

Results

Menadione strongly induces cytotoxicity in neuronal cells

The ability of menadione to induce cell death in cultured HT22 hippocampal neurons was analyzed by using different methods. The MTT assay showed that treatment of HT22 cells with menadione strongly induced, in a concentration-dependent manner, the loss of cell viability, with an IC_{50} of ~6 μM (Fig. 1A). Similarly, flow cytometric analyses of menadione-treated HT22 cells stained with PI alone or PI+annexin V-FITC showed that menadione increased the population of annexin V-positive cells (Fig. 1B) and DNA-fragmented cells (Figs. 1C, D), in a concentration-dependent manner. Notably, when the remaining live cell population was analyzed for cell cycle composition, the relative cell populations in the G_0/G_1, S, and G_2/M phases were not appreciably altered by treatment with menadione (Figs. 1E, F).

Menadione induces mitochondrial oxidative stress and dysfunction in neuronal cells

First, we examined mitochondrial accumulation of superoxide in menadione-treated neuronal cells. After the cells were treated with 4 or 8 μM menadione for 4 h, cells were stained with MitoSOX Red, a mitochondrial superoxide-specific dye. Treatment with menadione markedly increased the levels of mitochondrial superoxide. Accumulation of superoxide in the mitochondria was abrogated by co-treatment of cells with *N*-acetyl-cysteine (NAC), an antioxidant (Fig. 2A), and the decrease in the mitochondrial superoxide levels was accompanied by a reduction in the loss of cell viability (Fig. 2B).

Next, we determined the changes in mitochondrial membrane potential (MMP) following treatment with menadione. After the cells were treated with 8 μM menadione for 12 or 24 h, they were stained with $DiOC_6(3)$, an indicator of MMP, and analyzed by flow cytometry.

Menadione lowered the MMP in a time-dependent manner (Fig. 2C). To obtain more direct evidence to show that menadione causes mitochondrial damage, we investigated the mitochondrial morphological changes using the transmission electron microscopy (TEM). Following treatment with menadione, a significant fraction of the mitochondria became swollen and lost cristae (Fig. 2D). The relative population of the damaged mitochondria was increased in a time-dependent manner (Fig. 2E). Together, these data show that menadione causes mitochondrial superoxide accumulation and damage.

Menadione-induced neuronal death is caspase 3-independent

Based on the observations that menadione can induce the exposure of phosphatidylserine on the outer surface of cells (Fig. 1B), DNA fragmentation (Figs. 1C, D), and mitochondrial dysfunction and damage (Figs. 2C, D), it appears that menadione may induce the mitochondrion-dependent apoptotic cell death in cultured HT22 cells. To determine the exact mechanism by which menadione induces cell death in these cells, we examined the potential role of caspase-3 activation and the subsequent poly-(ADP-ribose) polymerase (PARP) cleavage by using Western immunoblotting. We found that neither caspase-3 cleavage (the activated form) nor PARP cleavage could be detected in neuronal cells when they were treated with 8 μM menadione for 24 h (Fig. 3A). Notably, when the caspase 3 activation was measured at several earlier time points (4, 8, and 12 h) after menadione treatment, there was no appreciable activation detected either (data not shown). By contrast, when these cells were treated with etoposide (a topoisomerase II inhibitor that can induce typical apoptotic cell death in many cell types), caspase-3 activation and PARP cleavage were clearly detected (Fig. 3A), suggesting that the caspase 3-dependent apoptotic pathway is functionally intact in these cells.

To confirm that caspase-3 (along with other caspases) is not involved in menadione-induced neuronal death, next we pre-treated neuronal cells with or without a pan-caspase inhibitor (z-VAD-fmk) and then co-incubated cells with 8 μM menadione. As shown in Fig. 3B, the Trypan blue exclusion assay showed that the pan-caspase inhibitor had no appreciable protective effect against menadione-induced cell death. Similarly, flow cytometric analysis also showed that the pan-caspase inhibitor could not prevent neuronal cells from undergoing menadione-induced cell death (Fig. 3C). By contrast, the cell death induced by 50 μM etoposide was strongly suppressed by the pan-caspase inhibitor under the same experimental conditions (Fig. 3B).

It is known that the activation of caspase-9, which subsequently activates caspase-3, requires ATP for apoptosome formation (Hu et al., 1999; Li et al., 1997). To determine whether the lack of caspase-3 activation is due to a rapid, early depletion of cellular ATP resulting from menadione-induced mitochondrial oxidative damage and dysfunction, we examined the time-dependent changes in intracellular ATP levels following menadione treatment. ATP levels were found to be decreased in a time-dependent manner, with nearly 80% of the cellular ATP depleted at 8 h after menadione treatment (Fig. 3D).

Lastly, we also compared the nuclear morphological changes seen during the development of the caspase-independent neuronal death with those characteristic changes commonly associated with caspase-dependent cell death. It was noted that although the nuclear size was reduced in menadione-treated cells, which was similar to what was seen in cells undergoing caspase-dependent apoptosis, chromatin condensation was basically absent in these cells (Fig. 3E; MD). In comparison, when neuronal cells were treated with etoposide, typical chromatin condensation could be readily observed (Fig. 3E; ETP).

Role of AIF and Endo G in menadione-induced neuronal death

To determine how menadione induces hippocampal cell death in a caspase-independent manner, we investigated whether the cell death is mediated by the apoptosis-inducing factor (AIF) and/or endonuclease G (Endo G), both of which can induce DNA fragmentation and subsequent cell death independently of caspase 3 and ATP. We found that AIF, Endo G, and cytochrome *c* were all detected in the cytosolic fraction after menadione treatment (Figs. 4A, B). In addition, AIF and Endo G were both translocated into the nucleus (Fig. 4C), consistent with their role in catalyzing DNA fragmentation. In comparison, only cytochrome *c* was released into the cytoplasm after etoposide treatment (Fig. 4A).

To investigate whether AIF and Endo G release from mitochondria contributes to menadione-induced cell death, we first knocked down these molecules individually. As shown in Fig. 4D, AIF and Endo G expression levels were significantly suppressed following transfection with specific siRNAs for each. Under this condition, cells were then treated with menadione for 12 h. Cells with selective AIF or Endo G knockdown were only partially resistant to menadione-induced cell death (Fig. 4E). Next, we jointly knocked down both AIF and Endo G in these cells (Fig. 4F). In the double-knockdown cells, menadione-induced cell death was significantly protected at 12 h after menadione treatment, but this protection was lost at 24 h (Fig. 4G).

Together, these data suggest that the menadione-induced DNA fragmentation in neuronal cells is independent of ATP and caspase-3, but it is mediated by AIF and Endo G. Because the mitochondria are extensively damaged as a result of excess mitochondrial superoxide accumulation (shown in Fig. 2), even a joint knockdown of AIF and Endo G still could not effectively prevent the menadione-treated cells from undergoing death at later time points.

Role of mitochondrial superoxide dismutase in menadione-induced neuronal death

Previously, we have reported that the mitochondrial superoxide dismutase (SOD2) plays an important role in protecting HT22 neuronal cells against glutamate-induced oxidative stress and cell death (Fukui and Zhu, 2010). Here we further investigated the effect of SOD2 over-expression or selective knockdown on menadione-induced oxidative stress and cell death. Neuronal cells that over-expressed SOD2 were treated with 8 μM menadione for 4 h, and then the cells were stained with MitoSOX Red, a mitochondrial superoxide-specific dye. The accumulation of mitochondrial superoxide was found to be markedly reduced in SOD2-overexpressing cells compared to the empty vector-transfected cells (Fig. 5A). Quantitative analysis of mitochondrial superoxide accumulation was performed using flow cytometry (Fig. 5B). In addition, when the SOD2-overexpressing cells were treated with menadione for 24 h, they were significantly more resistant to menadione-induced cell death (Fig. 5C). In comparison, cells with a selective and stable knockdown of either SOD1 or SOD2 became more susceptible to menadione-induced cytotoxicity (Fig. 5D). Notably, cells with a selective SOD2 knockdown were significantly more sensitive to menadione cytotoxicity compared to cells with a selective SOD1 knockdown (Fig. 5D).

Role of MAPKs in mediating menadione-induced neuronal death

It has been extensively documented that oxidative stress can result in the activation of the mitogen-activated protein kinase (MAPK) signaling pathways (*i.e.*, JNK, p38, and ERK), which then lead to apoptosis (Saitoh et al., 1998). Hence, we have also examined in this study the role of JNK, p38, and ERK in mediating menadione-induced apoptotic cell death in HT22 hippocampal neurons. All three MAPKs were found to be activated (phosphorylated) within 15–60 min following menadione treatment (Fig. 6A). However, none of the pharmacological inhibitors of these three MAPKs, namely, SP600125 for JNK1/2, SB202190 for p38, and PD98059 for ERK1/2, appreciably prevented these cells

from menadione-induced oxidative cytotoxicity (MTT assay; Figs. 6B, C, D). The lack of a protective effect of MAPK inhibitors was also noted when morphological changes of the treated cells were examined (data not shown). Notably, we recently have reported that these same inhibitors for JNK, p38, and ERK exerted a strong protective effect in HT22 neuronal cells during glutamate-induced oxidative cytotoxicity (Fukui et al., 2009). Taken together, these data indicate that the MAPK signaling pathways, while activated by menadione treatment, are not the predominant signaling pathways that eventually result in cell death.

Discussion

Using the HT22 mouse hippocampal neurons as an *in vitro* model, we demonstrated in this study that treatment of these cells with menadione can preferentially induce mitochondrial oxidative stress and dysfunction, and ultimately, a distinct form of cell death. Some of the features of the cell death induced by menadione are summarized in Table 1, which are discussed and explained below. In addition, we found that while SOD2 over-expression strongly protects these neurons against menadione-induced cell death, suppression of SOD2 expression sensitizes them to menadione-induced cytotoxicity.

It has been reported that caspase activation contributes to menadione-induced apoptosis in MCF-7 cells (Akiyoshi et al., 2009) and rat cerebral cortical neurons (Tripathy and Grammas, 2009). In pancreatic cells, menadione causes the release of cytochrome *c* from mitochondria to cytoplasm and activation of capase-9 and caspase-3 (Gerasimenko et al., 2002). However, the results of our present study showed that while preferential mitochondrial superoxide accumulation induced by menadione does induce mitochondrial cytochrome *c* release into cytoplasmic compartment, it does not activate caspase 3 nor PARP. It is known that activation of caspase-9, which then activates caspase-3, requires ATP as well as cytochrome *c* for apoptosome formation (Hu et al., 1999; Li et al., 1997). We observed in this study that the intracellular ATP levels are markedly reduced at 4 h after treatment with menadione, and >80% depletion is seen at 12 h. Therefore, it is evident that the absence of caspase-3 activation in menadione-treated neuronal cells is largely due to rapid mitochondrial superoxide accumulation and damage which subsequently depletes intracellular ATP levels.

To understand how mitochondrial superoxide generation causes DNA fragmentation and cell death in a caspase-3-independent manner, we sought to examine the role of endonucleases. There are three major endonucleases, *i.e.,* caspase-activated DNase (CAD), AIF, and Endo G. Because CAD activation requires the function of activated caspases (Nagata et al., 2003), it was deemed unlikely to be involved in mediating the death of HT22 hippocampal cells. Therefore, we chose to focus on examining the contribution of AIF and Endo G, both of which are ATP-independent endonucleases. We found that these two molecules are translocated following menadione treatment from the mitochondria to cytoplasmic compartment and then to the nucleus. However, knockdown of these two molecules using specific siRNAs fails to permanently protect the cells against menadione-induced cytotoxicity. This result is not surprising because it is expected that the mitochondria of these cells are so severely damaged that their ability to synthesize ATP will be largely destroyed. Even though the levels of these two endonucleases are markedly reduced following their knockdowns, which are expected to slow down DNA fragmentation during the process of cell death, cells still cannot survive for long due to the lack of mitochondrial function and ATP. Notably, there is another endonuclease named DNase-gamma, which belongs to the DNase I family and can also contribute to DNA fragmentation in an ATP-independent manner during cell death (Shiokawa and Tanuma, 2004). Since we found that the HT22 neuronal cells did not express this endonuclease (data not shown), its potential contributing role in menadione-induced cell death was thus not further examined.

In this study, we showed that SOD2 over-expressing cells are highly resistant to menadione-induced cytotoxicity, but cells with SOD2 knockdown become highly susceptible to its cytotoxicity compared to control cells (with normal SOD2 level). Although superoxide can spontaneously dismute to hydrogen peroxide in the absence of SOD2, it is estimated that the presence of SOD2 may drastically increase the rate of its conversion, thereby preventing superoxide from reducing transition metals and also reducing the chances for hydroxyl radical formation. The formed hydrogen peroxide in the mitochondria of neuronal cells can be converted to water by a number of enzyme systems. An earlier study showed that the thioredoxin/peroxiredoxin system, which uses GSH as reducing cofactor, plays a major role in the conversion of mitochondrial hydrogen peroxide to water in neuronal cells (Drechsel and Patel, 2010; Murphy, 2009). In addition, the glutathione peroxidase/reductase system also contributes, to a significantly smaller extent, to the reduction of hydrogen peroxide (Drechsel and Patel, 2010; Murphy, 2009). It is generally thought that catalase may play a minimal role in the detoxification of the mitochondrial hydrogen peroxide during oxidative stress in neuronal cells.

A recent study has reported the ability of menadione to induce cell cycle arrest and cell death in cancer cells (Lamson and Plaza, 2003). In the present study, we showed that menadione did not appreciably induce cell cycle arrest in cultured HT22 cells (Fig. 1D). The possibility cannot be ruled out that menadione may have a different modulating effect on the cell cycle in different types of cells.

For many years, two cell death pathways, namely, apoptosis and necrosis, have been considered as the main forms of cell death. Apoptosis is a form of programmed cell death during development, homeostasis and disease, whereas necrosis is commonly regarded as an accidental unregulated form of cell death. There is cumulating evidence suggesting that the execution of necrotic cell death is also under precise regulatory controls involving various signaling pathways (Festjens et al., 2006; Golstein and Kroemer, 2007). Some researchers have proposed the term ‘necroptosis’ or ‘paraptosis’ as a regulated necrosis (as opposed to the accidental necrosis) (Christofferson and Yuan, 2010; Sperandio et al., 2000; Vandenabeele et al., 2010; Zhang et al., 2009). As summarized in Table 1, the results of our present study demonstrate that the overall features of cell death induced by preferential mitochondrial superoxide generation are distinctly different from those of apoptosis. Caspase-independency, rapid depletion of ATP levels, release of AIF and Endo G from the mitochondria, and swelling of mitochondria, are among the notable features that appear to resemble necroptosis. The results of this study show that early, rapid disruption of the mitochondrial ATP production is an important underlying factor in the induction of necroptosis-like cell death in neuronal cells.

Lastly, it is of note that autophagy, a highly-regulated cellular mechanism for degradation of long-lived proteins and dysfunctional organelles, has been implicated in various neurological diseases (Banerjee et al., 2010; Son et al., 2012; Xilouri and Stefanis, 2010). Whereas excessive autophagy may result in cell death under certain conditions, the basal or stress-induced autophagy also has distinct cytoprotective functions. It will be of considerable interest in the future to explore the potential role of autophagy in modulating the severity of neuronal cell death resulting from oxidative damage to cellular organelles, particularly the mitochondria.

Conclusion

As depicted in Fig. 7, the metabolism of menadione by one-electron reducing enzymes leads to the formation of an unstable semi-quinone radical, which is further reduced to the stable hydroquinone (Iyanagi and Yamazaki, 1970). Reverse oxidation of the unstable

semiquinone generates superoxide radical ($O_2^{\bullet -}$) when molecular oxygen is present. Mitochondrial dysfunction caused by excess mitochondrial superoxide decreases intracellular ATP levels, and also causes the release of cytochrome c and caspase-independent cell death inducers, such as AIF and Endo G. Because of the rapid depletion of cellular ATP as a result of mitochondrial dysfunction, caspase activation is not initiated during the process of menadione-induced neuronal cell death. Instead, AIF and Endo G released from mitochondria jointly contribute to DNA fragmentation in the absence of caspase activation. Induction of the mitochondrial SOD2 effectively catalyzes mitochondrial superoxide to hydrogen peroxide, which alleviates mitochondrial oxidative stress and injury and thereby protects neuronal cells from necroptosis. Hydrogen peroxide is further detoxified by the thioredoxin/peroxiredoxin and peroxidase/reductase systems.

Abbreviations

SOD	superoxide dismutase
ROS	reactive oxygen species
MMP	mitochondrial membrane potential
AIF	apoptosis-inducing factor
Endo G	endonuclease G

References

Akiyoshi T, Matzno S, Sakai M, Okamura N, Matsuyama K. The potential of vitamin K3 as an anticancer agent against breast cancer that acts *via* the mitochondria-related apoptotic pathway. Cancer Chemother. Pharmacol. 2009; 65:143–150. [PubMed: 19449007]

Banerjee R, Beal MF, Thomas B. Autophagy in neurodegenerative disorders: pathogenic roles and therapeutic implications. Trends Neurosci. 2010; 33:541–549. [PubMed: 20947179]

Behl C, Skutella T, Lezoualc'h F, Post A, Widmann M, Newton CJ, Holsboer F. Neuroprotection against oxidative stress by estrogens: structure-activity relationship. Mol. Pharmacol. 1997; 51:535–541. [PubMed: 9106616]

Chance B, Sies H, Boveris A. Hydroperoxide metabolism in mammalian organs. Physiol. Rev. 1979; 59:527–605. [PubMed: 37532]

Christofferson DE, Yuan J. Necroptosis as an alternative form of programmed cell death. Curr. Opin. Cell Biol. 2010; 22:263–268. [PubMed: 20045303]

Clark, DD.; Sokoloff, L.; Siegel, GJ.; Agranoff, BW.; Albers, RW.; Fisher, SK.; Uhler, MD., editors. Basic Neurochemistry: Molecular, Cellular and Medical Aspects. Lippincott; Philadelphia: 1999. p. 637-670.

Connor KM, Subbaram S, Regan KJ, Nelson KK, Mazurkiewicz JE, Bartholomew PJ, Aplin AE, Tai YT, Aguirre-Ghiso J, Flores SC, Melendez A. Mitochondrial H_2O_2 regulates the angiogenic phenotype *via* PTEN oxidation. J. Biol. Chem. 2005; 280:16916–16924. [PubMed: 15701646]

Coyle JT, Puttfarcken P. Oxidative stress, glutamate, and neurodegenerative disorders. Science. 1993; 262:689–695. [PubMed: 7901908]

Criddle DN, Gillies S, Baumgartner-Wilson HK, Jaffar M, Chinje EC, Passmore S, Chvanov M, Barrow S, Gerasimenko OV, Tepikin AV, Sutton R, Petersen OH. Menadione-induced reactive oxygen species generation *via* redox cycling promotes apoptosis of murine pancreatic acinar cells. J. Biol. Chem. 2006; 281:40485–40492. [PubMed: 17088248]

Drechsel DA, Patel M. Respiration-dependent H_2O_2 removal in brain mitochondria *via* the thioredoxin/peroxiredoxin system. J. Biol. Chem. 2010; 285:27850–27858. [PubMed: 20558743]

Festjens N, Vanden Berghe T, Vandenabeele P. Necrosis, a well-orchestrated form of cell demise: signalling cascades, important mediators and concomitant immune response. Biochim. Biophys. Acta. 2006; 1757:1371–1387. [PubMed: 16950166]

Fukui M, Zhu BT. Mitochondrial superoxide dismutase SOD2, but not Cytosolic SOD1, plays a critical role in protection against glutamate-induced oxidative stress and cell death in HT22 neuronal cells. Free Radic. Biol. Med. 2010; 48:821–830. [PubMed: 20060889]

Fukui M, Song JH, Choi JY, Choi HJ, Zhu BT. Mechanism of glutamate-induced neurotoxicity in culture HT22 cells. Eur. J. Pharmacol. 2009; 617:1–11. [PubMed: 19580806]

Gerasimenko JV, Gerasimenko OV, Palejwala A, Tepikin AV, Petersen OH, Watson AJ. Menadione-induced apoptosis: roles of cytosolic Ca(2+) elevations and the mitochondrial permeability transition pore. J. Cell Sci. 2002; 115:485–497. [PubMed: 11861756]

Golstein P, Kroemer G. Cell death by necrosis: towards a molecular definition. Trends Biochem. Sci. 2007; 32:37–43. [PubMed: 17141506]

Halliwell B. Reactive oxygen species and the central nervous system. J. Neurochem. 1992; 59:1609–1623. [PubMed: 1402908]

Hanaichi T, Sato T, Iwamoto T, Malavasi-Yamashiro J, Hoshino M, Mizuno N. A stable lead by modification of Sato's method. J. Electron Microsc. 1986; 35:304–306.

Hu Y, Benedict MA, Ding L, Núñez G. Role of cytochrome c and dATP/ATP hydrolysis in Apaf-1-mediated caspase-9 activation and apoptosis. EMBO J. 1999; 18:3586–3595. [PubMed: 10393175]

Iyanagi T, Yamazaki I. One-electron-transfer reactions in biochemical systems. V. Difference in the mechanism of quinone reduction by the NADH dehydrogenase and the NAD(P)H dehydrogenase (DT-diaphorase). Biochim. Biophys. Acta. 1970; 216:282–294. [PubMed: 4396182]

Kudin AP, Bimpong-Buta NY, Vielhaber S, Elger CE, Kunz WS. Characterization of superoxide-producing sites in isolated brain mitochondria. J. Biol. Chem. 2004; 279:4127–4135. [PubMed: 14625276]

Lamson DW, Plaza SM. The anticancer effects of vitamin K. Altern. Med. Rev. 2003; 8:303–318. [PubMed: 12946240]

Li P, Nijhawan D, Budihardjo I, Srinivasula SM, Ahmad M, Alnemri ES, Wang X. Cytochrome c and dATP-dependent formation of Apaf-1/caspase-9 complex initiates an apoptotic protease cascade. Cell. 1997; 14:479–489. [PubMed: 9390557]

Lin MT, Beal MF. Mitochondrial dysfunction and oxidative stress in neurode-generative diseases. Nature. 2006; 443:787–795. [PubMed: 17051205]

Maher P, Davis JB. The role of monoamine metabolism in oxidative glutamate toxicity. J. Neurosci. 1996; 16:6394–6401. [PubMed: 8815918]

Maier CM, Chan PH. Role of superoxide dismutases in oxidative damage and neurodegenerative disorders. Neuroscientist. 2002; 8:323–334. [PubMed: 12194501]

Murphy MP. How mitochondria produce reactive oxygen species. Biochem. J. 2009; 417:1–13. [PubMed: 19061483]

Nagata S, Nagase H, Kawane K, Mukae N, Fukuyama H. Degradation of chromosomal DNA during apoptosis. Cell Death Differ. 2003; 10:108–116. [PubMed: 12655299]

Nunomura A, Perry G, Aliev G, Hirai K, Takeda A, Balraj EK, Jones PK, Ghanbari H, Wataya T, Shimohama S, Chiba S, Atwood CS, Petersen RB, Smith MA. Oxidative damage is the earliest event in Alzheimer disease. J. Neuropathol. Exp. Neurol. 2001; 60:759–767. [PubMed: 11487050]

Saitoh M, Nishitoh H, Fujii M, Takeda K, Tobiume K, Sawada Y, Kawabata M, Miyazono K, Ichijo H. Mammalian thioredoxin is a direct inhibitor of apoptosis signal-regulating kinase (ASK) 1. EMBO J. 1998; 17:2596–2606. [PubMed: 9564042]

Shiokawa D, Tanuma S. Differential DNases are selectively used in neuronal apoptosis depending on the differentiation state. Cell Death Differ. 2004; 11:1112–1120. [PubMed: 15167901]

Smith MA, Perry G, Richey PL, Sayre LM, Anderson VE, Beal MF, Kowall N. Oxidative damage in Alzheimer's. Nature. 1996; 382:120–121. [PubMed: 8700201]

Sompol P, Ittarat W, Tangpong J, Chen Y, Doubinskaia I, Batinic-Haberle I, Abdul HM, Butterfield DA, St Clair DK. A neuronal model of Alzheimer's disease: an insight into the mechanisms of oxidative stress-mediated mitochondrial injury. Neuroscience. 2008; 153:120–130. [PubMed: 18353561]

Son JH, Shim JH, Kim KH, Ha JY, Han JY. Neuronal autophagy and neuro-degenerative diseases. Exp. Mol. Med. 2012; 44:89–98. [PubMed: 22257884]

Sperandio S, de Belle I, Bredesen DE. An alternative, nonapoptotic form of programmed cell death. Proc. Natl. Acad. Sci. U. S. A. 2000; 97:14376–14381. [PubMed: 11121041]

Thor H, Smith MT, Hartzell P, Bellomo G, Jewell SA, Orrenius S. The metabolism of menadione (2-methyl-1,4-naphthoquinone) by isolated hepatocytes. J. Biol. Chem. 1982; 257:12419–12425. [PubMed: 6181068]

Tripathy D, Grammas P. Acetaminophen inhibits neuronal inflammation and protects neurons from oxidative stress. J. Neuroinflammation. 2009; 6:10. [PubMed: 19291322]

Trushina E, McMurray CT. Oxidative stress and mitochondrial dysfunction in neurodegenerative diseases. Neuroscience. 2007; 145:1233–1248. [PubMed: 17303344]

Vandenabeele P, Galluzzi L, Vanden Berghe T, Kroemer G. Molecular mechanisms of necroptosis: an ordered cellular explosion. Nat. Rev. Mol. Cell Biol. 2010; 11:700–714. [PubMed: 20823910]

White EJ, Clark JB. Menadione-treated synaptosomes as a model for post-ischaemic neuronal damage. Biochem. J. 1988; 253:425–433. [PubMed: 3178721]

Xilouri M, Stefanis L. Autophagy in the central nervous system: implications for neurodegenerative disorders. CNS Neurol. Disord. Drug Targets. 2010; 9:701–719. [PubMed: 20942791]

Xu X, Chua CC, Kong J, Kostrzewa RM, Kumaraguru U, Hamdy RC, Chua BH. Necrostatin-1 protects against glutamate-induced glutathione depletion and caspase-independent cell death in HT-22 cells. J. Neurochem. 2007; 103:2004–2014. [PubMed: 17760869]

Zhang DW, Shao J, Lin J, Zhang N, Lu BJ, Lin SC, Dong MQ, Han J. RIP3, an energy metabolism regulator that switches TNF-induced cell death from apoptosis to necrosis. Science. 2009; 325:332–336. [PubMed: 19498109]

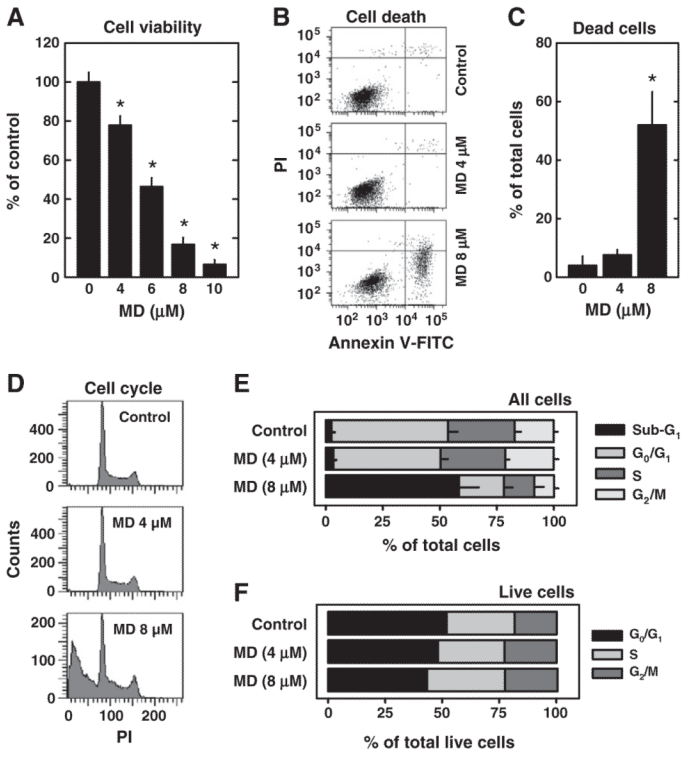

Fig. 1.

Menadione (MD) induces cell death and DNA fragmentation in neuronal cells. A. HT22 cells were treated with menadione at indicated concentrations for 24 h. The cell viability was determined using the MTT assay. Values are the mean±S.D. of three experiments. **P*<0.05 *vs* control. B and C. HT22 cells were treated with 4 or 8 μM menadione for 24 h. Cells were stained with annexin V-FITC and PI as described in Materials and methods, and were analyzed using flow cytometry. The quantitative data for the annexin V-positive cells (±S.D.) are shown in panel C. D–F. HT22 cells were treated with 4 or 8 μM menadione for 24 h. Cells were fixed and stained with PI to analyze the cell cycle changes as described in Materials and methods. The quantitative values for the relative populations of cells in different phases of the cell cycle are shown in E, and the relative populations of cells among all live cells (*i.e.*, excluding dead cells) are shown in F. The populations of cell cycle were calculated from three independent flow cytometric analyses.

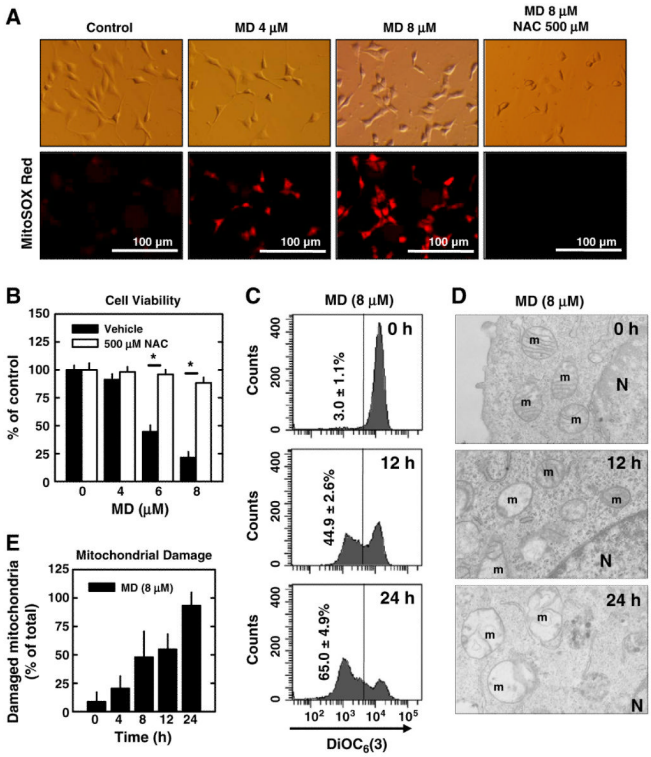

Fig. 2.

Menadione (MD) induces mitochondrial superoxide accumulation and dysfunction in neuronal cells. A. HT22 cells were pre-treated with/without 500 μM *N*-acetyl-cysteine (NAC) for 2 h and then co-incubated with menadione at indicated concentrations. After 4 h incubation, cells were stained with MitoSOX Red as described in Materials and methods. Digital images were captured under a fluorescence microscope (×200). B. HT22 cells were pre-treated with or without 500 μM NAC for 2 h and then co-incubated with menadione at indicated concentrations for additional 24 h. Cell viability was determined using the MTT assay. C. HT22 cells were treated with 8 μM menadione for 12 or 24 h. Cells were then stained with 25 nM $DiOC_6(3)$ as described in Materials and methods, and the mitochondrial membrane potential was analyzed using flow cytometry. D. HT22 cells were treated with 8 μM menadione for 8 or 24 h and then cells were fixed and subjected to transmission electron microscope (TEM) analysis as described in Materials and methods. m: mitochondrion; N: nucleus. E. The quantitative data for the damaged mitochondria based on the TEM analysis. Values are the mean±S.D. of three experiments. * $P<0.05$ *vs* the corresponding control.

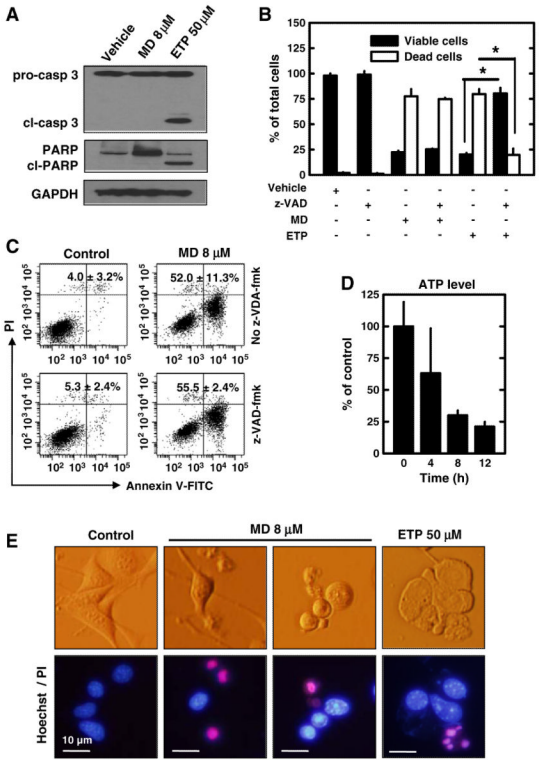

Fig. 3.

Menadione (MD) induces caspase-independent cell death in neuronal cells. A. HT22 cells were treated with 8 μM menadione or 50 μM etoposide (ETP) for 24 h. Cell extracts were prepared and subjected to Western blotting of PARP and caspase-3. Membranes were stripped and re-probed for GAPDH as a loading control. Shown are results from a representative experiment. B. HT22 cells were pre-treated with/without 20 μM z-VAD-fmk for 2 h and then co-incubated with 8 μM menadione or 50 μM etoposide (ETP) for 24 h. Live and dead cells were determined using the Trypan blue exclusion assay. C. HT22 cells were pre-treated with/without 20 μM z-VAD-fmk for 2 h and then co-incubated with 8 μM menadione for 24 h. Then cells were stained with annexin V-FITC and PI as described in Materials and methods. Cells were analyzed by flow cytometry. The average ratio of annexin V-positive cells (±S.D.) was calculated from three experiments. D. HT22 cells were treated with 8 μM menadione for the indicated length of time. Intracellular ATP levels were measured and normalized to untreated cells. E. Nuclear morphological changes in HT22 cells treated with menadione for 12 h or etoposide (ETP) for 24 h were observed after Hoechst-33342 and PI double staining. Values are the mean±S.D. of three experiments. ** $P<0.05$ *vs* the corresponding control.

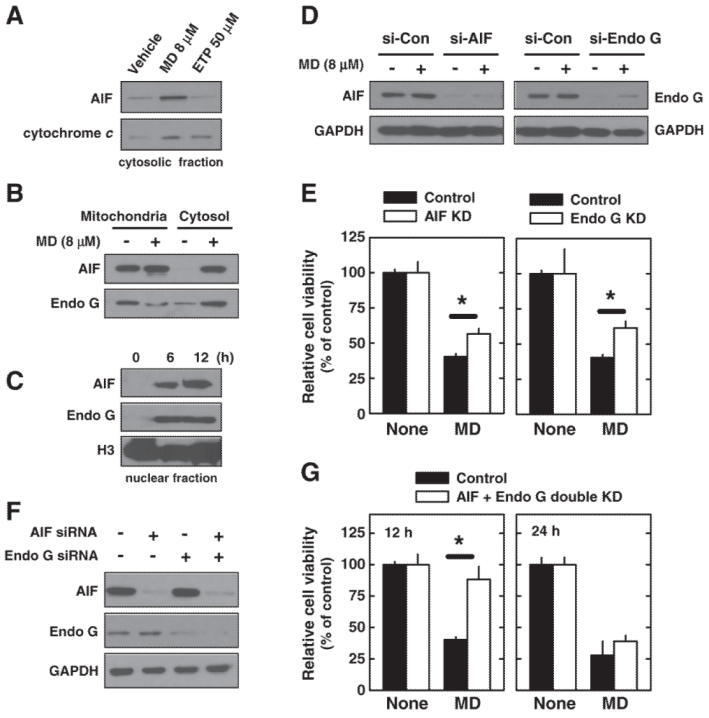

Fig. 4.

Menadione (MD) induces AIF and Endo G release from mitochondria in neuronal cells. A. HT22 cells were treated with 8 μM menadione for 12 h or with 50 μM etoposide (ETP) for 24 h. Then cytosol fraction was isolated and cell extracts were subjected to Western blotting of AIF and cytochrome *c*. B. HT22 cells were treated with 8 μM menadione for 12 h. Then mitochondria and cytosol fractions were isolated and cell extracts were subjected to Western blotting of AIF and Endo G. C. HT22 cells were treated with 8 μM menadione for 6 or 12 h. Then nuclear fraction was isolated and cell extracts were subjected to Western blotting of AIF and Endo G. Histon H_3 (H3) was shown as an internal control. D and E. HT22 cells were transfected with specific siRNAs for AIF and Endo G. Twenty-four h later, cells were treated with 8 μM menadione and further incubated for 12 h. Protein expression was confirmed by Western blotting (D). Cell viability was determined by the MTT assay (E). F and G. HT22 cells were transfected with specific siRNAs in specific combination as indicated. Twenty-four h later, cells were treated with 8 μM menadione and further incubated for 12 or 24 h. Protein expression was confirmed by Western blotting (F). Cell viability was determined by the MTT assay (G). Values are the mean±S.D. of three experiments.

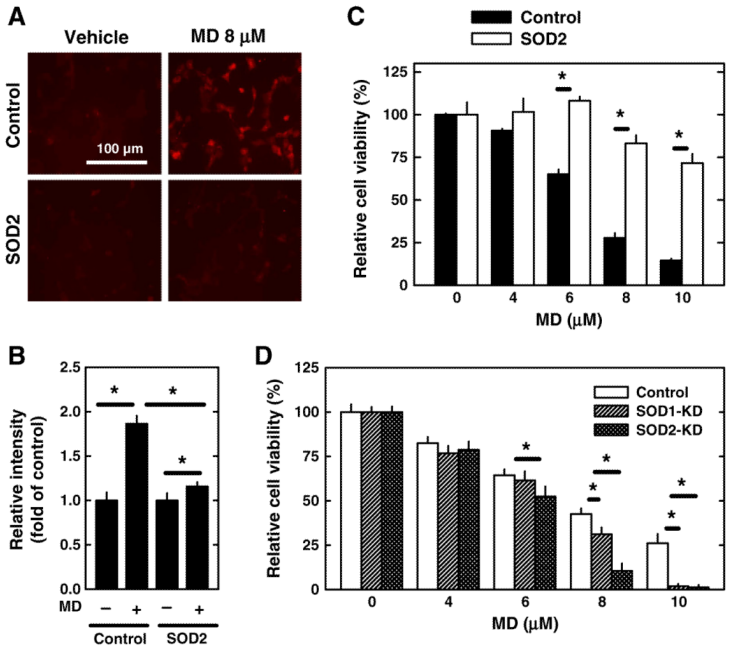

Fig. 5.

Effect of SOD2 expression levels on menadione (MD)-induced neuronal cell death. A–B. Control HT22 cells and SOD2-overexpressing HT22 cells were treated with 8 μM menadione for 4 h. Accumulation of mitochondrial superoxide was determined by MitoSOX Red staining and quantified using flow cytometry as described in Materials and methods. Values are the mean±S.D. of three experiments. C. Control HT22 cells and SOD2-overexpressing HT22 cells were treated with menadione at indicated concentrations for 24 h. D. Control HT22 cells and HT22 cells with selective knockdown of SOD1 or SOD2 were treated with menadione at indicated concentrations for 24 h. Cell viability was determined using the MTT assay. Values are the mean±S.D. of three experiments. * $P<0.05$ *vs* the corresponding control.

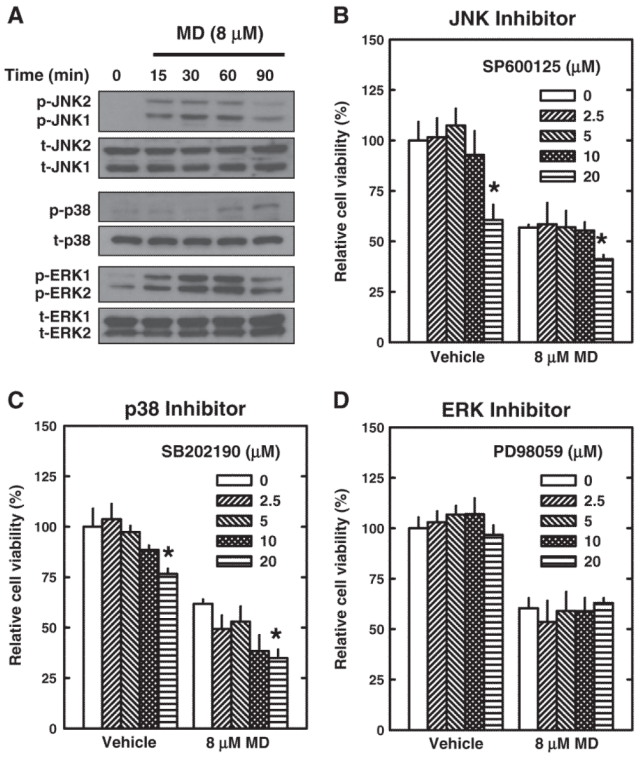

Fig. 6.

Effect of menadione (MD) on MAPK signaling pathways in neuronal cells. A. HT22 cells were treated with 8 μM menadione for indicated length of time. Cell extracts were prepared and subjected to Western blotting with antibodies specific for phospho-JNK, phospho-p38, or phospho-ERK. Membranes were stripped and re-probed for total-JNK, total-p38, or total-ERK as controls. B–D. HT22 cells were pre-treated with specific inhibitors of MAPKs (SP600125 for JNK, SB202190 for p38, and PD98059 for ERK) at indicated concentrations for 2 h and then co-incubated with 8 μM menadione for additional 24 h. Cell viability was determined by the MTT assay. Values are the mean±S.D. of three experiments. * $P<0.05$ *vs* the correspond control (without an inhibitor).

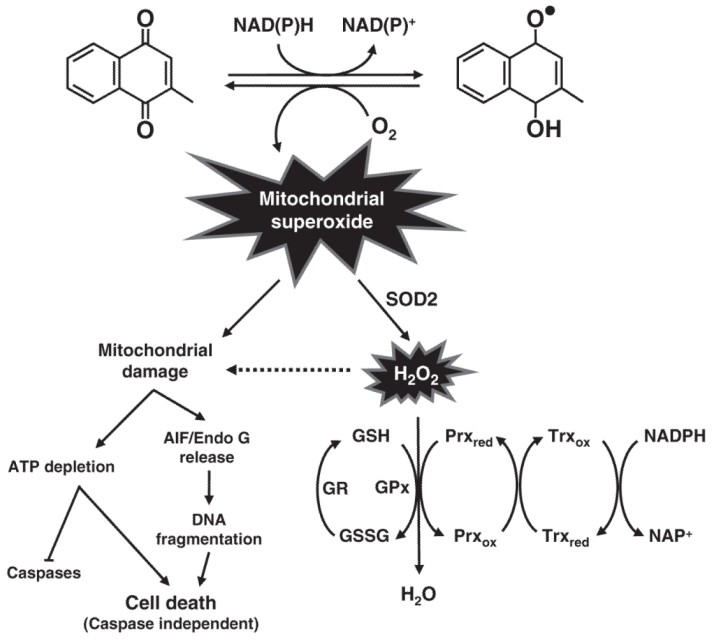

Fig. 7.

Schematic illustration of the mechanism of menadione-induced neurotoxicity in neuronal cells. Metabolism of menadione by one-electron reducing enzymes, such as microsomal NADPH-dependent cytochrome P450 reductase and mitochondrial NADH-dependent ubiquinone oxidoreductase, generates an unstable radical metabolite. Reverse oxidation generates ROS ($O_2^{\bullet -}$) when molecular oxygen is present. Mitochondrial dysfunction caused by mitochondrial superoxide decreases intracellular ATP levels, and releases caspase-independent apoptosis inducers AIF and EndoG. Higher level of mitochondrial SOD2 can effectively catalyze mitochondrial superoxide to hydrogen peroxide. Hydrogen peroxide is further detoxified mostly by the thioredoxin/peroxiredoxin system in the mitochondria of neuronal cells. Besides, the glutathione peroxidase/reductase system also contributes to the reduction of hydrogen peroxide. Abbreviations: GSH, glutathione; GSSG, glutathione disulfide; Prx, peroxiredixins; Trx, thioredoxin-2; GPx, glutathione peroxidases; GR, glutathione reductase.

Table 1

Comparison of features between classical apoptosis and mitochondrial superoxide-induced neuronal cell death.

	Classical apoptosis	Mitochondrial superoxide-induced neuronal cell death
• Loss of plasma membrane asymmetry	Yes	Yes
• Mitochondrial permeability change	Yes	Yes
• Rapid mitochondrial swelling and damage	No	Yes
• Cytochrome C release	Yes	Yes
• Dependence on cellular ATP	Yes	No
• DNA fragmentation	Yes	Yes
• DNA fragmenting enzymes involved		
Caspases 3/9 activation	Yes	No
Caspase-activated DNase (CAD)	Yes	No
AIF	No	Yes
EndoG	No	Yes